Bethan Warren[1*], Gregory J. Hunt[2†], Michael Bryant[1], Anne Neville[1], Ardian Morina[1], Michael Gahagan[2]

[1] Institute of functional surfaces, School of Engineering, Leeds University, LS2 9JT, UK
[2] Lubrizol Limited, The Knowle, Nether Lane, Hazelwood, Derby DE56 4AN, UK
*Corresponding author, email: bethan@djwarren.co.uk
†Email: Gregory.hunt@lubrizol.com

Automatic transmission fluid corrosion inhibitor interactions with copper

Abstract

In this paper a new method, measuring the change in resistance of a thin copper wire, has been applied to provide a way to monitor the reaction in situ. Two different corrosion inhibitors used in commercial ATFs, have been studied using this new test method coupled with a more traditional coupon test to allow surface analysis to be carried out at 110 ℃, 120 ℃, 130 ℃ and 150 ℃. Both inhibitors were found to be equally as effective up to temperatures of 130 ℃, however the evidence provided shows that at 150 ℃ the thiadiazole inhibitor is breaking down leading to severe pitting on the surface. Corrosion performance cannot be assumed to be effective at all temperatures and the current method provides a convenient quantitative screening method for inhibitor evaluation.

Key Words: Corrosion inhibitor, thiadiazole, OBT, resistance change

1. Introduction

In recent years there has been a drive towards the electrification of vehicles, whereby electrical components, primarily made of copper alloys, are introduced into the gearbox [1]. This addition of copper containing materials that are added not just for a mechanical function, such as bushings, seals or brazings but are connected via electronics means that the compatibility of copper with automatic transmission fluids is an important concern which must be considered when automatic transmission fluid (ATF) additives are developed. As well as providing specific functional properties, such as minimising wear and lubricating gears, to name but a few, the ATF must not adversely interact with copper surfaces.

The most common way to evaluate the amount of corrosion caused by an ATF to a copper surface is using the standard ASTM D130 test method which compares a copper test coupon, which has been immersed in an ATF for a number of hours, to a set of standards and a rating is given based on the colour only, [2]. There are a number of issues regarding the suitability of this test, the first being that it was originally designed to test the corrosiveness of petroleum products (base oil) to copper. The second is that this test gives a visual rating only and provides no information as to what is happening at the surface. Expansion of the test to include analysis of copper in solution does little to address these concerns.

There are few studies which look at the interaction of copper specifically with ATFs [3]–[5]. ATFs are complex chemical formulations with multiple competing interactions and understanding the basic individual additive component interactions with copper surfaces merits further study. ATF additives include: corrosion inhibitors, dispersants, detergents, antioxidants, friction modifiers and antiwear additives. The performance of an ATF requires multiple competing demands to be balanced. In order

to do this effectively, an understanding of the additive-additive and additive-surface interactions need to be obtained. A detailed understanding can aid in the development of new additives but also achieve improved performance through reformulation by minimising undesirable interactions.

This paper focuses on the interaction of two different oil soluble corrosion inhibitors with a copper surface at a range of temperatures, before looking at a combination of these two corrosion inhibitors. This study combines a variation of the ASTM D130 standard test method with a newer methodology for probing corrosion by measuring the change in resistance of a copper wire [6], [7] immersed in the fluid of interest, which can then be directly related to a change in the radius of the copper wire. The information is supported by advanced surface analytical techniques which elucidate the nature of the chemical films formed. This integration of surface analysis allows information to be gained that is not accessible with the ASTM D130 test method alone. This combined methodology, which includes ASTM ratings, wire radius changes and surface analysis, provides information regarding how the surface interaction may be progressing with time and allows a suggestion of the mechanisms that may be involved [8].

2. Experimental Details

2.1 Experimental Method

The method used combines both a simple coupon test and a wire resistance change test, both carried out in the same beaker. This allowed the process to be followed in situ, with the wire test, but giving easier analysis of the surface, using the copper coupon. A schematic of the setup along with a picture of the test wired up and ready for the start of the experiment are shown in Figure 1.
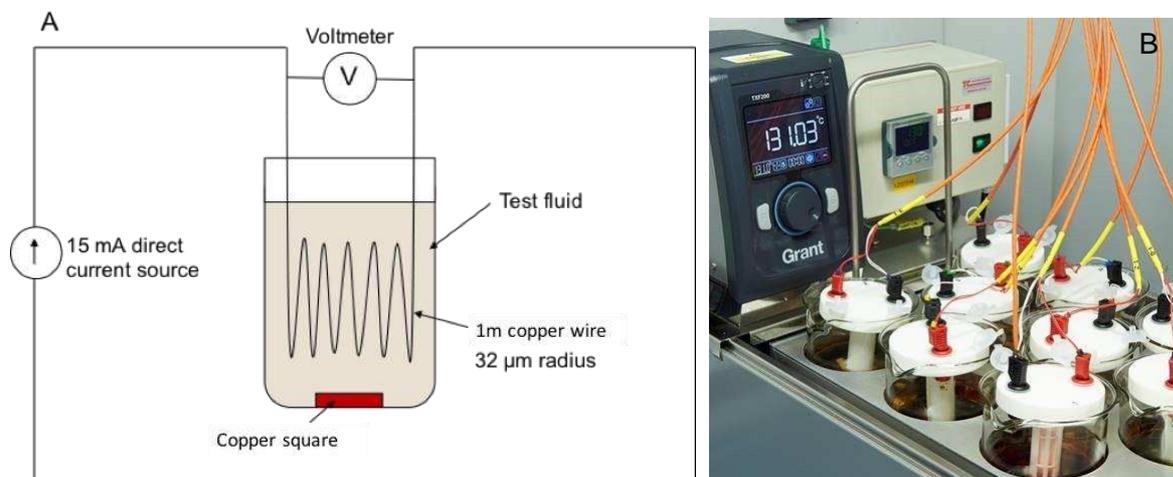
Figure 1 A. Schematic of wire and coupon in beaker of test fluid B. Photograph of beakers in thermostatically controlled oil bath during testing

A thermostatically controlled oil bath was preheated to the correct temperature, 110 ℃, 120 ℃, 130 ℃ or 150 ℃. The temperature of the oil in the b ath is recorded every 10 seconds along with the resistance of the wire. The accuracy of the temperature measurements is ± 0.15 ℃. Table 1 shows the temperature at which each test fluid was run, further information on the additives can be found in

Table **2**.

The test fluids were blended to the concentrations defined in

Table **2**. The fluids were shaken for approximately 20 seconds before each test to ensure sample homogeneity and approximately 400 mL of the test fluid was placed into a clean glass beaker.

Table 1 Test Fluid Temperatures

ATF additive tested	110 ℃	120 ℃	130 ℃	150 ℃
DMTD	✓	✓	✓	✓
OBT	✓	✓	✓	✓
Combination of DMTD and OBT		✓		✓

To follow the reactions in situ the resistance of a copper wire was measured periodically. This resistance measurement can be directly related to the radius using Ohms law, Equation 1. Where R = resistance of the wire in Ω; ρCu_T = resistivity of copper in Ωm at temperature T; l = length of wire in m and r = radius of copper in m.

Equation 1

$$R = \frac{\rho Cu_T l}{\pi r^2}$$

The resistiviy of the wire must first be calculated for each point to account for fluctuations in temperature, this is done using Equation 2, where ρCu_T = resitivity of copper to be calculated at temperature T; ρCu_{20} = resistivity of copper at 20 ℃ (1.68 x10^{-8} Ωm); T = temperature at specific point; α = coefficient of thermal expansion of copper (3.86 x10^{-3} ℃ $^{-1}$)

Equation 2

$$\rho Cu_T = \rho Cu_{20} + \alpha(T - 20)\rho Cu_{20}$$

In order to compare the results from different wires the length of wire is calculated at the start of the test from its resistance and its known initial radius using a rearrangement of Ohms law, Equation 3. This is done as the wires differ slightly in length. The wire used in these studies had an initial radius of 3.2 x10^{-5} m.

Equation 3

$$l = \frac{R \pi r^2}{\rho Cu_T}$$

After calculating the length of each wire at the start of the test the length of the wire can be normalised to 1.01 m. This means recalculating the resistance values at each point and allows us to compare the values to others, regadless of the difference in wire length. The normalisation is carried out using Equation 4, where R = resistacne in Ω; l = length of wire in m; and R_{norm} = resistance values in Ω, normalised to 1.01 m.

Equation 4

$$R_{norm} = \frac{1.01}{l} \times R$$

Having normalised all the resistance data to a length of 1.01 m the radius of the wire can be calculated at each point using another rearrangement of Ohms law, Equation 5.

Equation 5

$$r_{norm} = \sqrt{\frac{\rho Cu_T \times 1.01}{\pi R_{norm}}}$$

This technique is similar to that recently described by Hunt and Gahagan [6], [7], with some minor differences. A 1 metre length of temper annealed, 64 μm diameter, copper wire of 99.9% purity, was used as received from Advent Research Materials. This was wound around a 3D printed nylon former and each end soldered to an electrical contact point.

The resistance temperature detector (RTD) data acquisition module used in this experiment was not capable of the same level of accuracy at the 1 mA condition as that used by Hunt and Gahagan [6], [7], however the accuracy improved significantly with higher current levels. 15 mA current was chosen to run the experiments as this had no impact on the loss of radius of the wire or result in any ohmic heating of the wire.

A former is used to hold the wire in the test fluid, this is a 3D printed nylon structure with spindles spaced such that 1 metre of wire can be wound and held securely and maximise wire exposure to the test fluid. A wired former was placed into each of the beakers containing the test fluid and a copper coupon. The connection points, soldered at each end of the wire, were attached to a control system which passed 15 mA of current through each of the wires.

A schematic of the experiment and a picture of the beakers set up in the thermostatically controlled oil bath is presented in Figure 1.

A 5 minute stabilisation period was run to determine the resistance in the measurement wires before connecting the experimental copper wire into the circuit. The beakers containing the test fluid, coupons and wires attached to the control system, were then placed into the pre heated oil bath and the resistance of the wire recorded every 10 seconds for 335 hours. The accuracy of the resistance measurements for these experiments is $\pm$ 57.8 mΩ. The error for radius changes using these measurements has been calculated from repeat data to be $\pm$ 0.12 μm. At the end of the test the coupons were removed from the beakers, rinsed with SBP2L[1] and air dried before being weighed to measure their weight before the start of the experiment. The copper wires were unwound from the former and placed into sterile polythene bags.

2.2 Materials

---

[1] SBP2L is a solvent comprised of C6-C10 paraffins and cycloparaffins with low levels of aromatics and was used as purchased from Shell

Two different oil soluble corrosion inhibitors were used in this study, with four test fluids investigated;

1. Base oil
2. Base oil with 0.5 wt% of an alkyl dimercaptothiadiazole (DMTD) corrosion inhibitor
3. Base oil with 0.05 wt% of a triazole type (OBT) corrosion inhibitor
4. Base oil with 0.5 wt% DMTD and 0.05 wt% OBT

The base oil used throughout this study is a group III base oil containing <1% of shear stable polymethacrylate (PMA).

Table **2** provides a brief description of the corrosion inhibitors and the concentration used in this study. The concentration of the corrosion inhibitors studied reflects the highest level of these types of corrosion inhibitors likely to be found in traditional ATF formulations. It is well documented in literature that benzotriazole is a good corrosion inhibitor for the protection of copper in aqueous environments, so an oil soluble benzotriazole, OBT, was chosen for study to see if the same was true in oil based media. DMTD was chosen as it is a common corrosion inhibitor used in lubricating fluids [9]–[13].

Table 2 corrosion inhibitors tested, including a short description and structural image and the concentration tested

ATF additive	Description of additive	Concentration tested
DMTD	1,3,4-thiadiazole with substituted sulfur chains	0.5 wt%
OBT	oil soluble benzotriazole	0.05 wt%
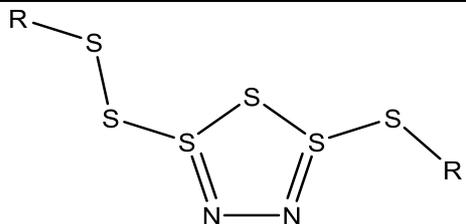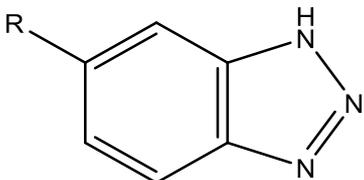
Copper coupons of 99.95% purity, provided by Metaspec, USA, were pre-cut into approximately 1 cm lengths. Each test used one copper coupon per beaker. The coupons were polished using cotton wool wetted with SBP2L and silicon carbide grit with an average diameter of 115 μm. The coupons were polished by hand for approximately 3 minutes on each side until a fresh copper surface was seen and visible signs of tarnish had been removed.

The coupons were then rinsed using SBP2L and weighed in grams using Mettler Toledo scales with an accuracy of 0.1 mg.

Weighed coupons were placed into the test fluid as quickly as possible to minimise oxidation of the surface. This allowed a clean surface to be produced which is still similar to those found in transmissions in real-life applications.

2.3 End of test analysis

Fluid analysis

Elemental analysis was performed at the end of the test on a portion of the used test fluid by inductively coupled plasma atomic emission spectroscopy (ICP-AES) to determine the amount of copper present. A Perkin Elmer ICP-AES system was used following the ASTM D5185 test method for used oils. The measurement uncertainty for the copper determinations using this experimental procedure is documented to be $0.12x^{0.91}$ where x is the ppm value of the copper present.

Surface analysis

After removal and rinsing of the coupons from the test fluid they were rated within an hour, using the ASTM D130 rating standards.

Scanning Electron Microscopy (SEM)

The surface films were investigated with a Hitachi TM3030 Scanning Electron Microscope (SEM) with an accelerating voltage of 15 kV.

Differential Scanning Calorimetry (DSC)

The DSC experiments were carried out using a Q2000 DSC from TA instruments.

White Light Interferometer

A non-contact Bruker NPFLEX was used.

XPS/X-ray Photoelectron Spectroscopy

The chemical analysis of the surface was performed using X-ray Photoelectron Spectroscopy (XPS) at NEXUS (National EPSRC XPS Users' Service), without further modification to the surface. Subsequent analysis was carried out using CasaXPS. All peaks were calibrated to the adventitious carbon peak at 284.8 eV. Peak positions were determined using the CasaXPS software with Gaussian-Lorentzian peak fitting and a Shirley background. A full width half maximum (FWHM) in the region of 1.6 – 1.8 was aimed for and peaks added or subtracted until both a good fit was achieved and the FWHM value was within the specified range.

3. Results and Discussion

The copper coupons run in each of the test fluids at each temperature were photographed and are shown in Table 3 with the ASTM rating also noted. Reproduction of the images in table 3 does not accurately describe the rating but Illustrates the differences.

The sample rating worsens as the temperature increases, as expected. What the ASTM test fails to capture is the differences in the surface. Taking samples immersed in DMTD as an example at 110 ℃, 120 ℃ and 130 ℃ they a re all rated as

3b, using the ASTM D130 rating method, yet the colour is steadily darkening and the range of colour present on the surface decreases with increasing temperature.

Reid and Smith [14] found that high levels of elemental sulfur in iso-octane gave rise to films of a dark grey/black colour that readily flaked away from the surface of copper. This appears to be similar to the sample in DMTD at 150 °C and XPS analysis has indicated high levels of sulfur on the surface, which are presented later.

Table 3 images of copper coupons after immersion in ATF additives for 335 hours with the corresponding ASTM rating

	110°C	120°C	130°C	150°C
Base oil	2e	2e	3a	4a
DMTD	3b	3b	3b	4c
OBT	1b	3a	3a	3a
Combination of corrosion inhibitors		3b		4a
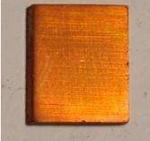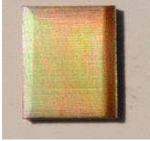
The resistance of a copper wire, immersed in a solution under investigation, was measured and from it the radius of the wire calculated. This allowed the change in radius of the copper wire to be measured with respect to time, giving a measurement of corrosion. As most of the changes are linear the end radius of the wire was taken in order to compare between fluids.
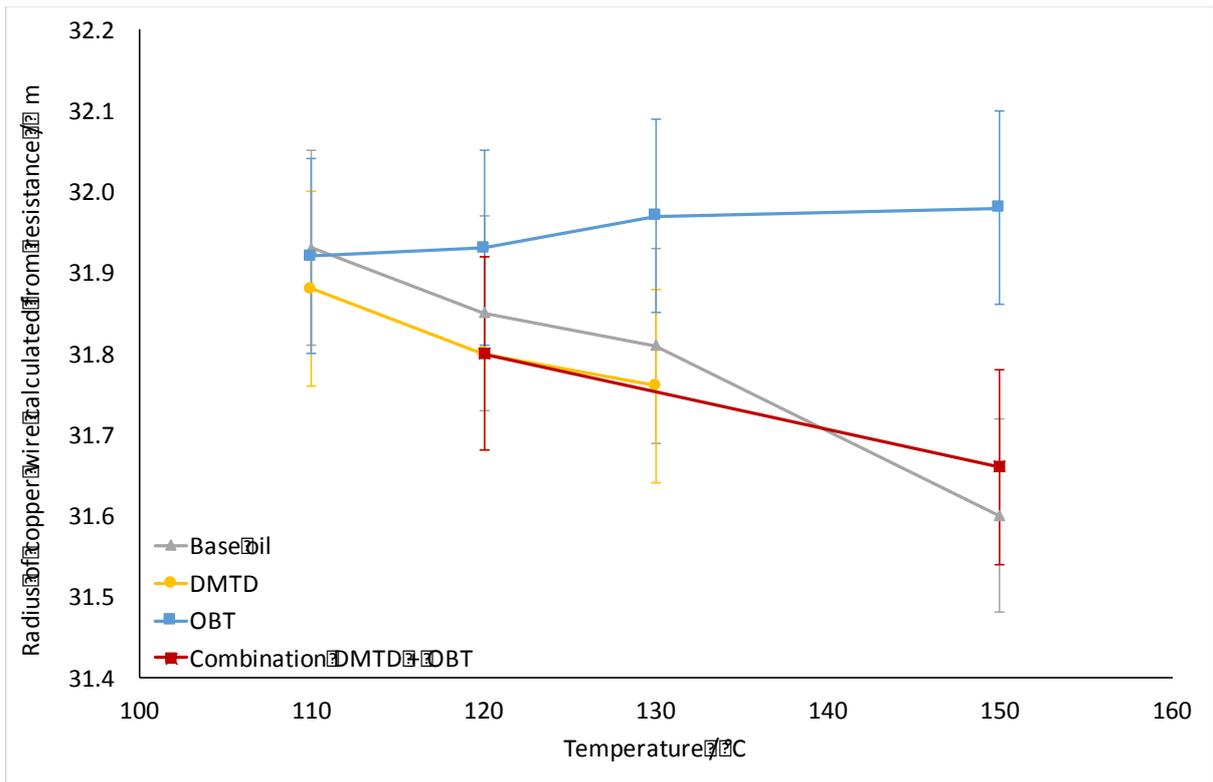
Figure **2** shows the final radius of the copper wire, calculated from its resistance after 335 hours, against temperature for each of the fluids under investigation.

The wire immersed in base oil shows a steadily decreasing radius with increasing temperature. This suggests that the base oil becomes slightly corrosive to copper, possibly as a result of oxidation products formed by the fluid over time.

The addition of OBT gives no measurable change in radius particularly at higher temperatures, suggesting that a more robust film is formed.
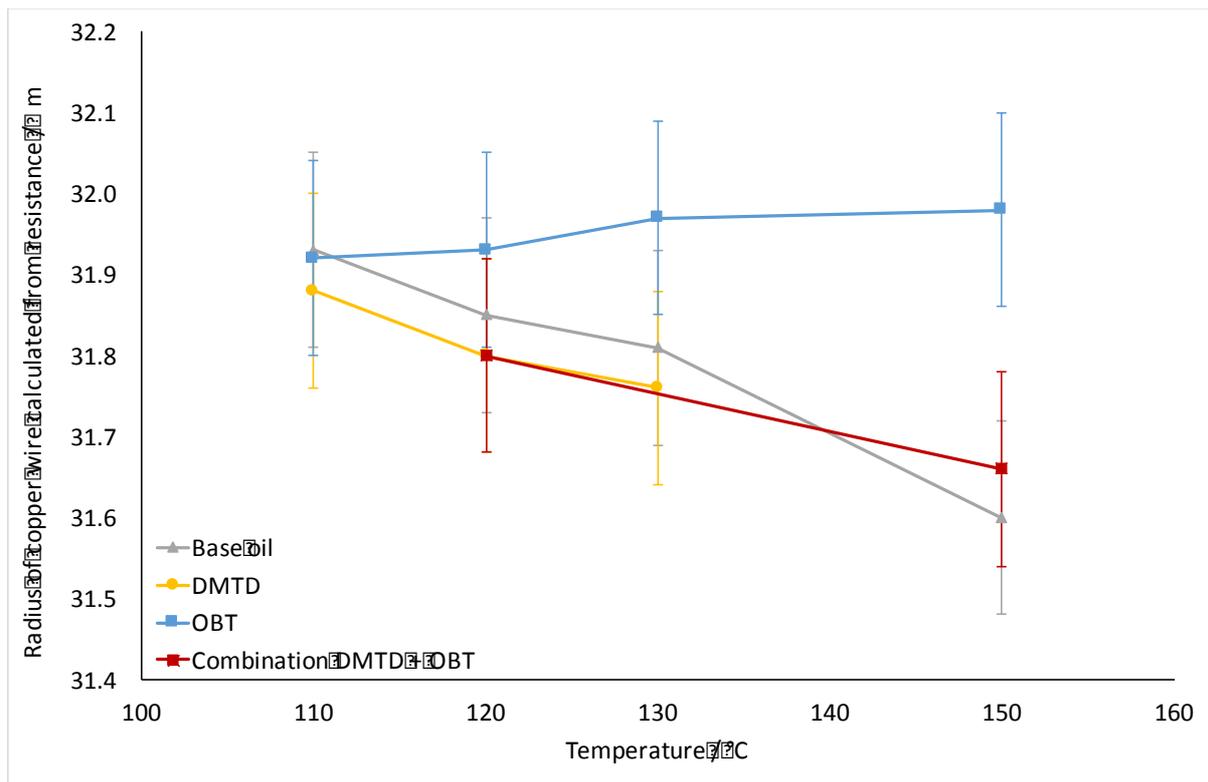
Figure 2 final radius of copper wire, calculated from resistance data, after 335 hours immersion in test fluid

For DMTD at 150 ℃ there is no radius plotted, this is because the wire broke, sending the resistance to infinity and consequently the calculated radius to 0. Since the wire had not completely dissolved there was still a radius present but this could not be calculated due to breakages in the wire. The wire was broken in 7 different places (11 during a repeat run) so it is clear that there is a different mechanism taking place at 150 ℃ causing DMTD to become corrosive towards copper. As the base oil tested alone does not show this behaviour it must be due to the presence of DMTD, rather than the formation of oxidation products in the base oil.

Figure 3 shows the change in radius of the copper wire over time at each of the four different temperatures for DMTD. At 150 ℃ after 50 hours the decrease in radius begins to accelerate, until approximately 130 hours where there is then a very rapid decrease in the radius, which lasts 2.5 hours at which point the wire breaks completely.

The combination of corrosion inhibitors at 120 ℃ has the same radius change as DMTD alone, however at 150 ℃ the wire did not break and so th e addition of OBT appears to have a beneficial impact.

It is clear that OBT is the least corrosive towards copper. Between the temperatures of 110 ℃ and 150 ℃ a difference between the corrosivit y of the base oil and DMTD is less certain. Comparison of the sample images in Table 3 show that DMTD is worse than the base oil, which follows the trend seen in the radius change data.
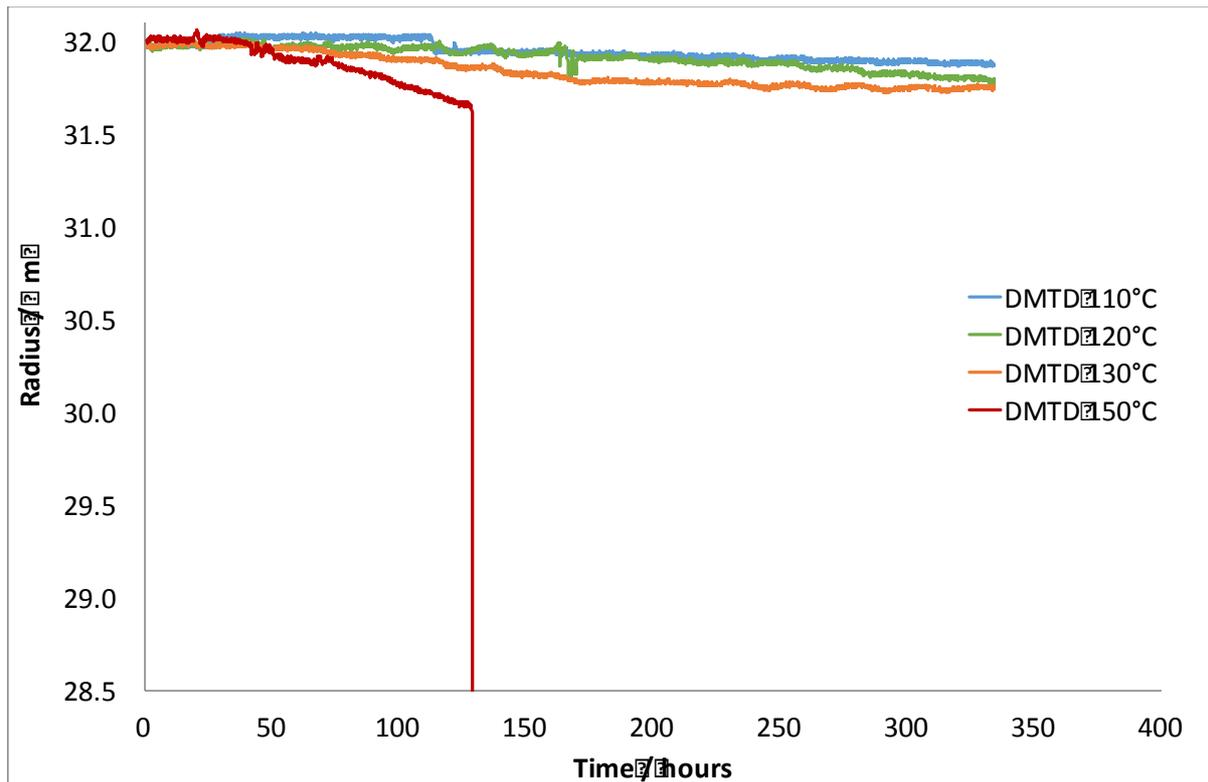
Figure 3 change in radius of copper wire immersed in DMTD at 110℃, 120℃, 130℃ and 150℃, over 335 hours

The amount of copper which has been dissolved in the ATF is measured at the end of test and is plotted in Figure 4. The copper measured in the base oil at the end of the test steadily increases with increasing temperature, correlating to the decrease in the radius of the copper wire. Similarly, the lack of radius change for the wire immersed in OBT is mirrored by the very low amounts of copper measured in the end of test OBT test fluid.

The low amount of copper measured for DMTD appears unusual given the results of the wire test. There is very little difference in the amount of copper measured in the end of test fluid between 120 ℃ and 150 ℃. Considering that in th e wire test at 150 ℃ the wire broke in several places it may be expected that the amount of copper should be high, but this is not the case. Pitting may be the cause of damage to the wire, and as they are often documented as being very small this explains why there is no real increase in the amount of copper measured in the end of test solution. It is however, possible that there is a loss of copper but it is insoluble and so although copper is lost from the surface it drops out of the fluid and is therefore not detected in the end of test fluid using ICP-AES.
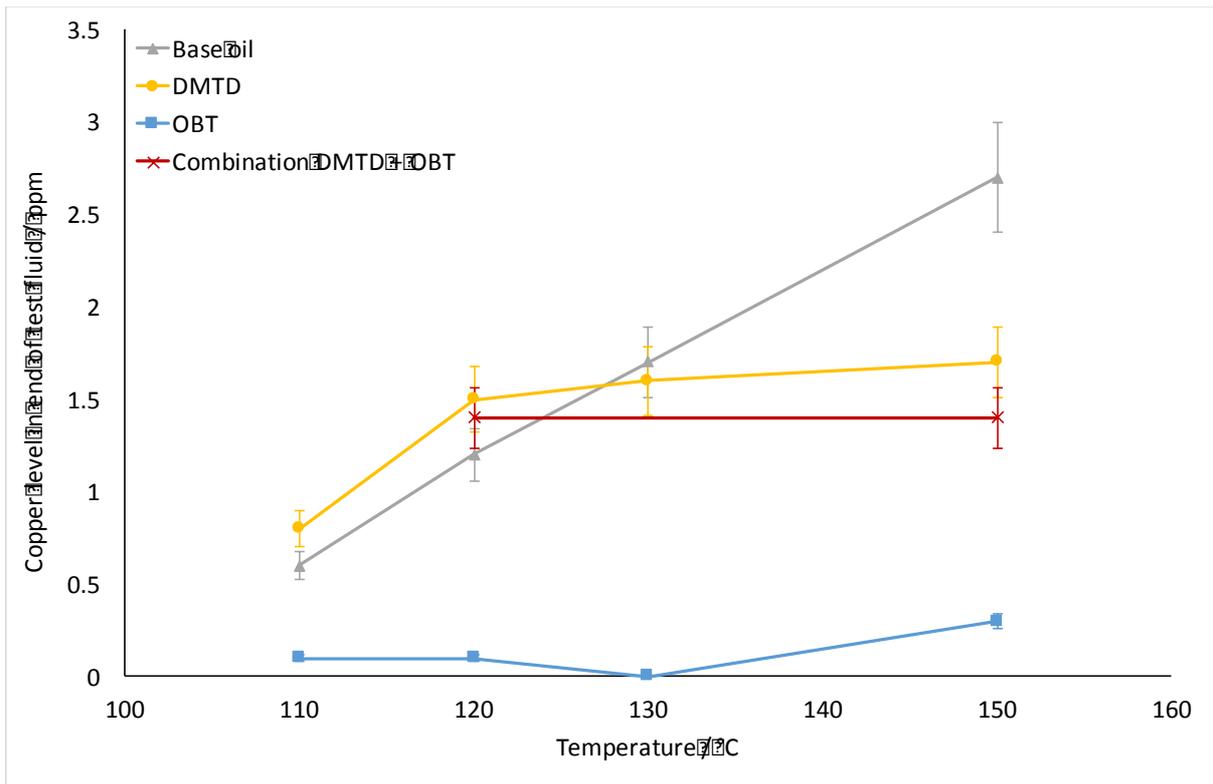
Figure 4 copper level in end of test fluid as determined by ICP-AES

In the wire test, there is clear evidence that the combination of corrosion inhibitors 1 and 2 is beneficial, in the fact the wire did not break at 150 ℃. The ICP-AES results show little difference between the amount of copper measured in the fluid with DMTD alone and the combination of both inhibitors. It is therefore important that all tests are considered before making a judgment on how well an additive performs.

There is a clear correlation between the decrease in radius of the copper wire and the amount of copper measured in the end of test fluid, as shown in
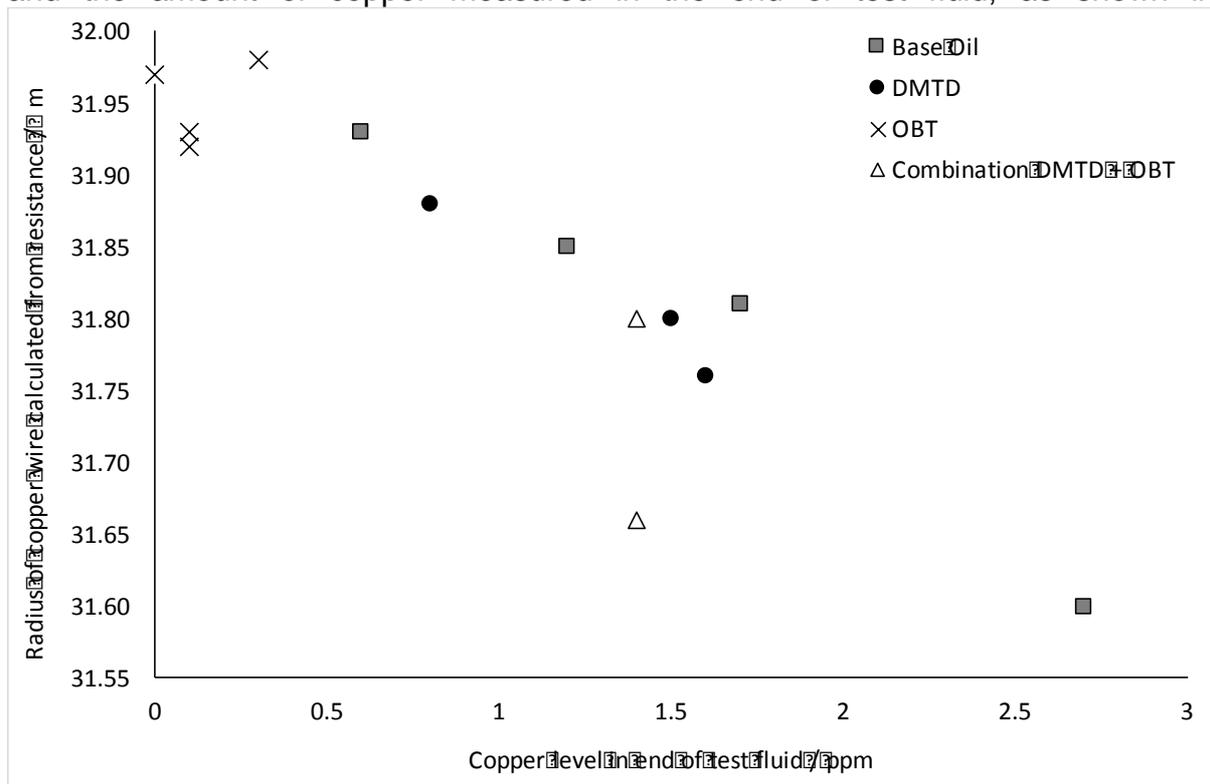
Figure **5**. This makes sense as we expect the wire test to indicate the amount of copper lost from the wire and the ICP-AES results to show how much copper has been dissolved into the fluid. Where there are deviations from this trend it is possible that the copper is being converted into a non- or lower conductive layer but is not necessarily being lost into the fluid.
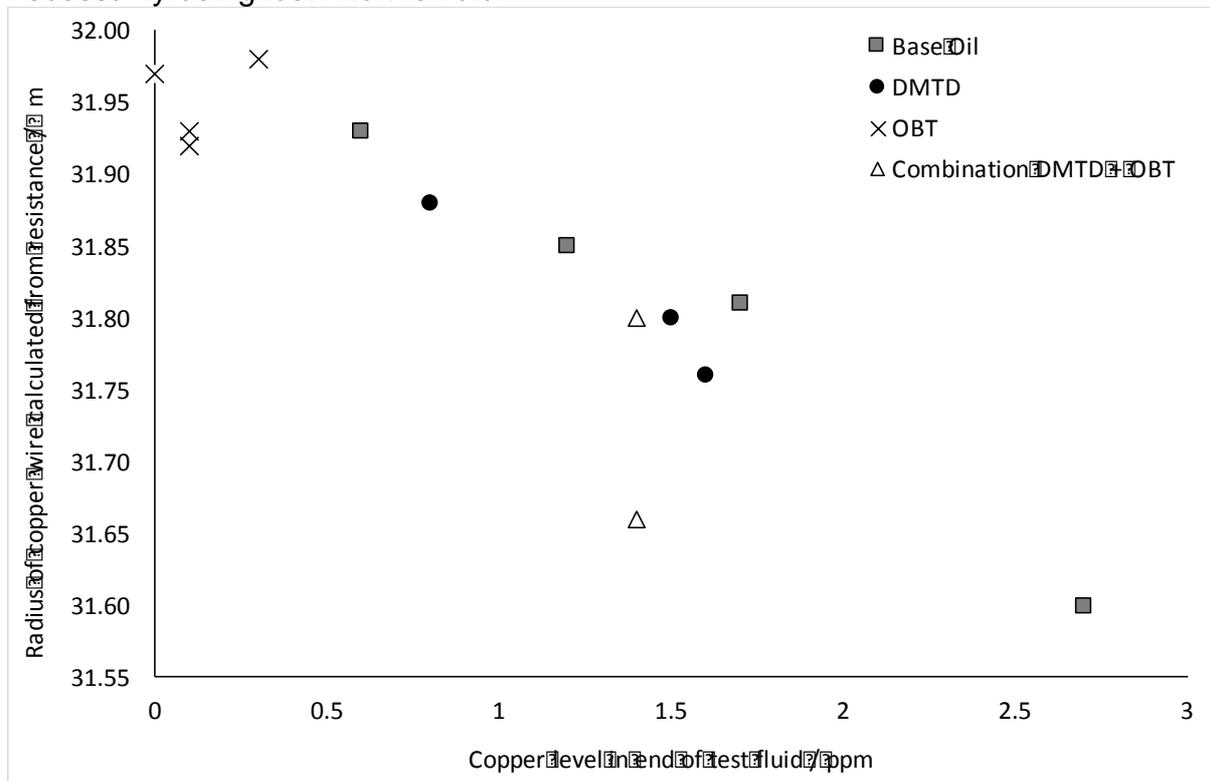
Figure 5 radius of copper wire at end of test plotted against the level of copper measured in the end of test fluid

3.2 Imaging and chemical analysis of coupon surfaces

Scanning Electron Microscopy (SEM) imaging was used to inspect the surface of the coupons which had been immersed in the test fluids. For the base oil, shown in Figure 6, there were similarities at 110 °C and 120 °C with no distinctive fe atures present on the surface. At 130 °C the surface was covered with some sort of deposit in the region of 5 μm – 10 μm in size. At 150 °C the deposit was much greater and had agglomerated in areas on the surface to give a flaking under layer with large particles on top in the region of 15 μm – 20 μm. These particles appear to be comprised of a number of smaller particles agglomerated together. It is thought that these may be oxidation products that have deposited out of the test fluid, although there is currently no clear evidence for this.

XPS analysis of the surfaces was conducted at 120 °C and 150 °C and similarities can be seen between the two spectra, as shown in Figure 7. The binding energies and percentage atomic concentration of each of the species identified in the spectra can be found in Table 4.
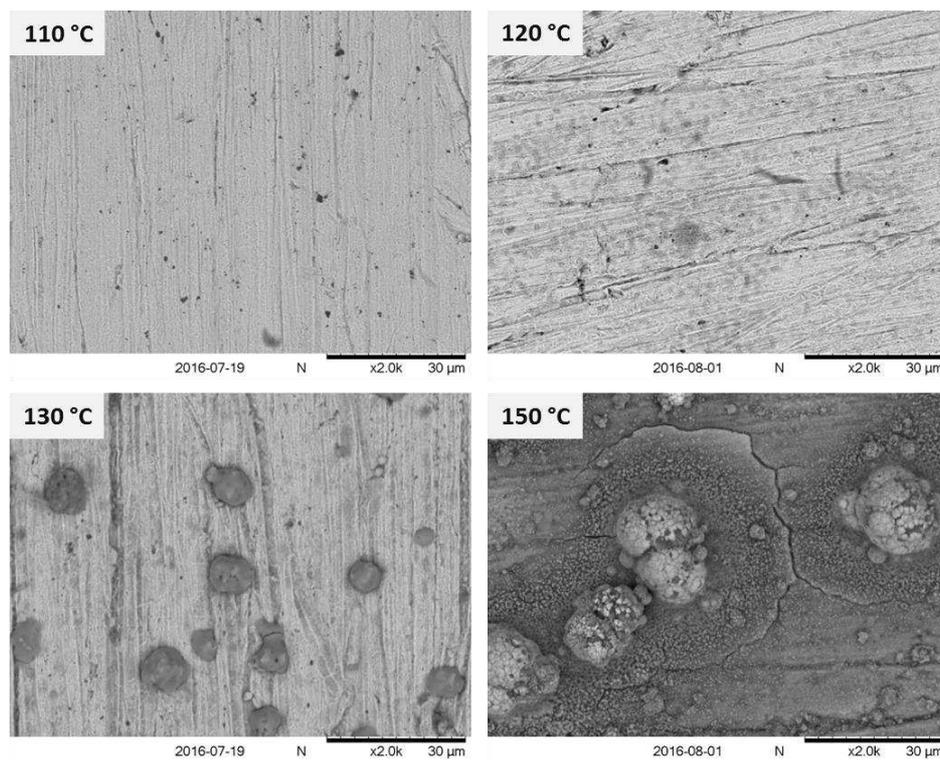
Figure 6 SEM images of the surface of copper coupons after 335 hours immersion in base oil at different temperatures
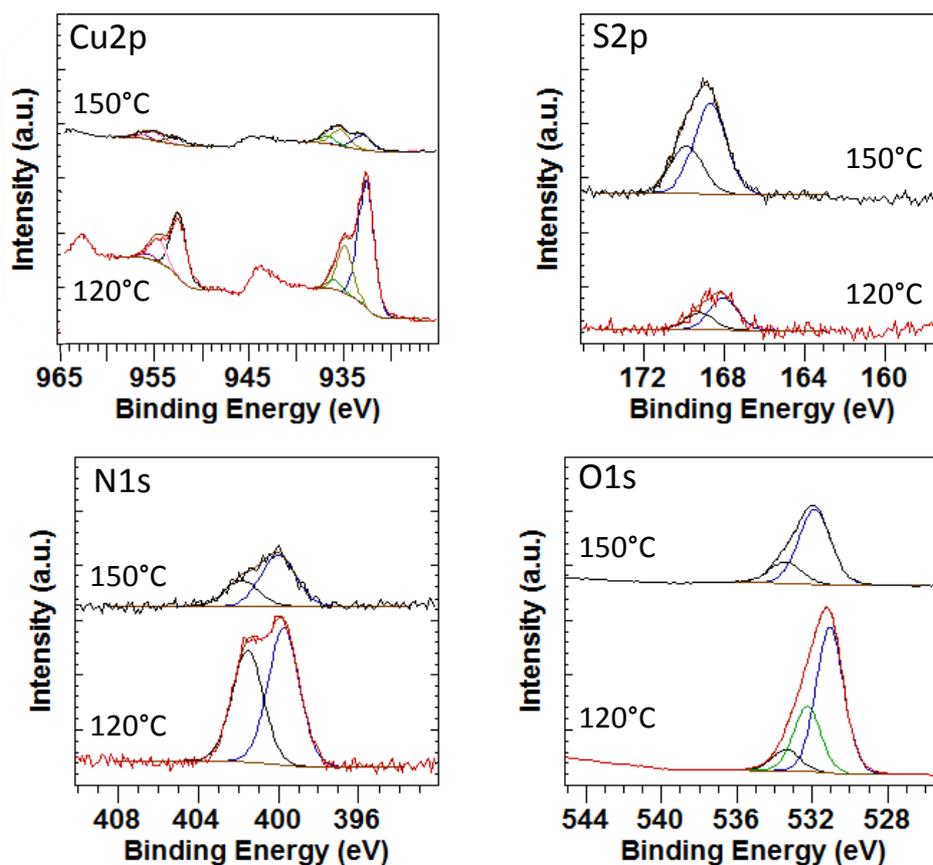
Figure 7 high resolution XPS spectra of the surface of copper coupons immersed base oil at 120 ℃ and 150 ℃

Table 4 XPS analysis of coupon after immersion in base oil for 335 hours

Peak	Species	120 ℃		150 ℃	
		Binding energy (eV)	% atomic concentration	Binding energy (eV)	% atomic concentration
C1s	C-C	284.82	55.96	284.82	64.82
C1s	C-O-C	286.35	8.84	286.52	9.62
C1s	O-C=O	288.41	3.89	288.55	5.22
O1s	Copper carbonate	531.07	14.02	531.80	11.84
O1s	C-O	532.20	9.50		
O1s	C=O	533.44	2.44	533.38	5.20
N1s		399.77	1.95	400.01	1.33
N1s		401.61	1.45	401.82	0.54
S2p$_{3/2}$	CuSO$_4$	168.01	0.30	168.42	0.71
Cu2p$_{3/2}$	Cu$_2$O/Cu$_2$S	932.69	0.68	932.86	0.10
Cu2p$_{3/2}$	CuO	934.91	0.27	934.85	0.09
Cu2p$_{3/2}$	CuSO$_4$	936.39	0.05	936.30	0.05

The percentage atomic concentration of copper at 150 ℃ is lower than a t 120 ℃. This is most likely due to the thickness of the layer on top of the cou pon. The depth of analysis for XPS is limited to around 5 nm, looking at the SEM images there are

larger particles on the surface of the 150 ℃, so it is feasible that they are m inimizing the amount of copper detected as the electrons will have to pass through them before being detected. However there are also likely to be spatial differences across the surface. For both samples the copper is in a Cu(II) oxidation state, which is identified from the satellite peaks present at ~945 eV and ~964 eV.

It can be seen that the level of oxygen is slightly lower at 150 ℃ w ith a lack of C-O present.

The level of sulfur is low for both samples but this should really be expected as the base oil should contain very low levels of sulfur (less than 0.03%).

Figure 8 shows SEM images of coupons which have been immersed in DMTD solution, with all temperatures showing signs of film formation. Between 110 °C and 130 ℃ small granular objects can be seen on the surface, particularly along what appear to be polishing marks. At 150 ℃ there is a very clear film coverin g the surface, which appears to be an agglomeration of smaller particles, with large agglomerates on the top almost like deposits. At 150 ℃ there was also some sev ere flaking in places where the film was completely removed from the surface. In these places the exposed copper showed very few polishing marks, suggesting that the reaction of the inhibitor with the surface incorporated the copper into the film. Interestingly the surface looks similar to those presented by Garcia-Anton et al. [15] where copper coupons were immersed into synthetic naphtha-containing different sulfur species.
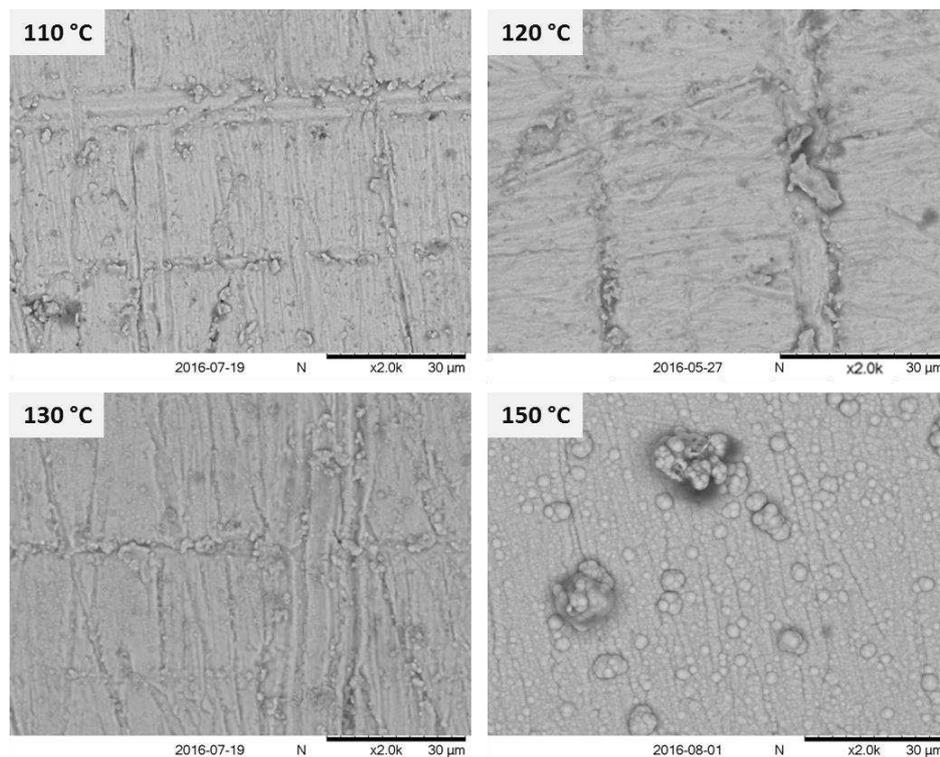
Figure 8 SEM images of the surface of copper coupons after 335 hours immersion in DMTD containing test fluid at different temperatures

XPS analysis for the surfaces at 120 ℃ and 150 ℃ showed som e significant differences. Table 5 lists the percentage atomic concentration for each of the species identified in the spectra and the corresponding binding energy. Figure 9 shows high resolution XPS spectra of the Cu $2p_{3/2}$, S $2p_{3/2}$, O 1s and N 1s peaks for samples previously immersed in DMTD solution at 120 ℃ and 150 ℃.

The first noticeable difference is that the copper is in a different oxidation state for each of the temperatures. For the 120 ℃ sample copper is in the Cu(II) oxidation state, whilst at 150 ℃ it is in the Cu(I) oxidation state. These oxidation states are differentiated by the presence, or lack, of satellite peaks at ~945 and ~964 eV. The most obvious difference about these states is the lack and presence of particular sulfur species. At 120 ℃ there is a large amount of $CuSO_4$ detected on the surface, with lesser amounts of Cu_2S. At 150 ℃ there is very little $CuSO_4$ detected but higher levels of Cu_2S. Reid and Smith [14] looked at the surface of copper coupons after undergoing the ASTM D130 test with different sulfur species. Their tests were carried out at 50 ℃ for three hours but they found with elemental sulfur and small chain thiols, copper peaks were consistent with a Cu(I) oxidation state, suggesting that after initial sulfur adsorption further growth of the surface film led to a Cu_2S film which was poorly adhered to the surface [14]. This is similar to the behaviour seen at 150 ℃ with DMTD, where a higher concentration of Cu_2S is seen on the surface. This suggests a breakdown of the side chains to give elemental sulfur or thiols, which then interact with the surface
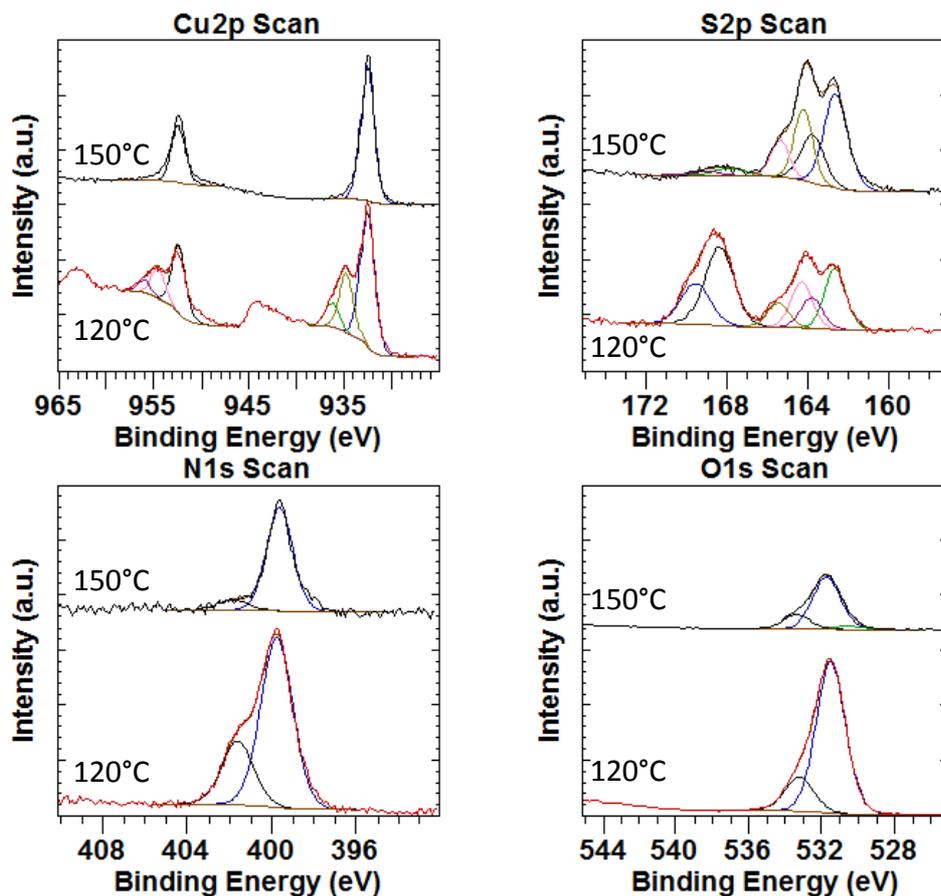
Figure 9 high resolution XPS spectra of the surface of copper coupons immersed in DMTD containing test fluid at 120 ℃ and 150 ℃

Table 5 XPS analysis of coupon after immersion in DMTD test solution for 335 hours

Peak	Species	120 ℃		150 ℃	
		Binding energy	% atomic concentration	Binding energy	% atomic concentration

C1s	C-C	284.82	44.03	284.83	70.01
C1s	C-O-C	286.41	9.19	286.39	6.70
C1s	O-C=O	288.48	3.76	288.56	3.54
O1s	Copper oxide/carbonate			530.66	1.89
O1s	C-O	531.41	26.43	531.80	7.13
O1s	C=O	533.15	4.68	533.41	1.72
N1s		399.77	3.28	399.52	2.09
N1s		401.59	1.68	401.87	0.36
S2p$_{3/2}$	Cu$_2$S	162.66	0.53	162.42	1.48
S2p$_{3/2}$	S/R-SH	164.29	0.46	164.08	0.91
S2p$_{3/2}$	CuSO$_4$	168.41	1.79	167.89	0.27
Cu2p$_{3/2}$	Cu$_2$O/Cu$_2$S	932.56	0.94	932.65	1.76
Cu2p$_{3/2}$	CuO	934.75	0.65		
Cu2p$_{3/2}$	CuSO$_4$	936.25	0.24		

.

At 150 °C there is a lack of oxygen at the surface of the sample. Th is is seen both in the decreased percentage atomic concentration and also in the S 2p$_{3/2}$ spectra where there is a very low intensity of the CuSO$_4$ peak. In the Cu 2p$_{3/2}$ spectra there are peaks corresponding to CuO and CuSO$_4$ at 120 °C which are not present in the 150 °C spectra. Reid and Smith [14] found that when ethanethiol and th iophenol were tested in the ASTM D130 test and the coupons then analysed by XPS an increase in sulfur concentration was accompanied by a gradual decrease in oxygen concentration. It is thought that the corrosion inhibitor molecule is breaking down at 150 °C giving short chain sulfur molecules, similar to those studied by Reid and Smith. The fact that the amount of oxygen is lower at 150 °C compared to at 1 20 °C, coupled with the fact that peaks consistent with CuS$_2$ and S/R-SH are greater at 150 °C suggests that the molecule does break down to form small chain sulfur molecules. A number of studies have shown that oils containing dibenzyl disulfide, which contains a similar sulfur chain linkage to DMTD, cause severe copper corrosion due to the presence of the sulfur chain [16]–[18].

Another noticeable difference is the change in the N 1s spectra in Figure 9. The nitrogen species present is difficult to identify. At 120 °C there are two distinct nitrogen environments, suggesting an asymmetrical structure, as expected from DMTD. At 150 °C there is only one dominant nitrogen environment. It is possible that the molecule is breaking down and losing the sulfur based side chains which would lead to a more symmetrical molecule and therefore 1 nitrogen environment.

In order to see if there was a difference in the breakdown of the molecule in the presence of copper DSC was carried out on two samples of 0.5 wt% DMTD in base oil. The first with only the corrosion inhibitor, and the second with a small amount of copper powder placed in the pan.

Figure 10 shows the results of the DSC scanned between 50 °C and 250 °C. It is clear that with copper present there is a decrease in the temperature at which the molecule breaks down. Without copper the temperature peak is at 193.8 °C, bu t when copper is present the temperature peak is at 176.9 °C. Both of these temp eratures are higher than 150 °C, the temperature at which the experiment is carried ou t, but it is possible that the extended time period of the experiment could have an impact, as could the local copper concentration at the surface.
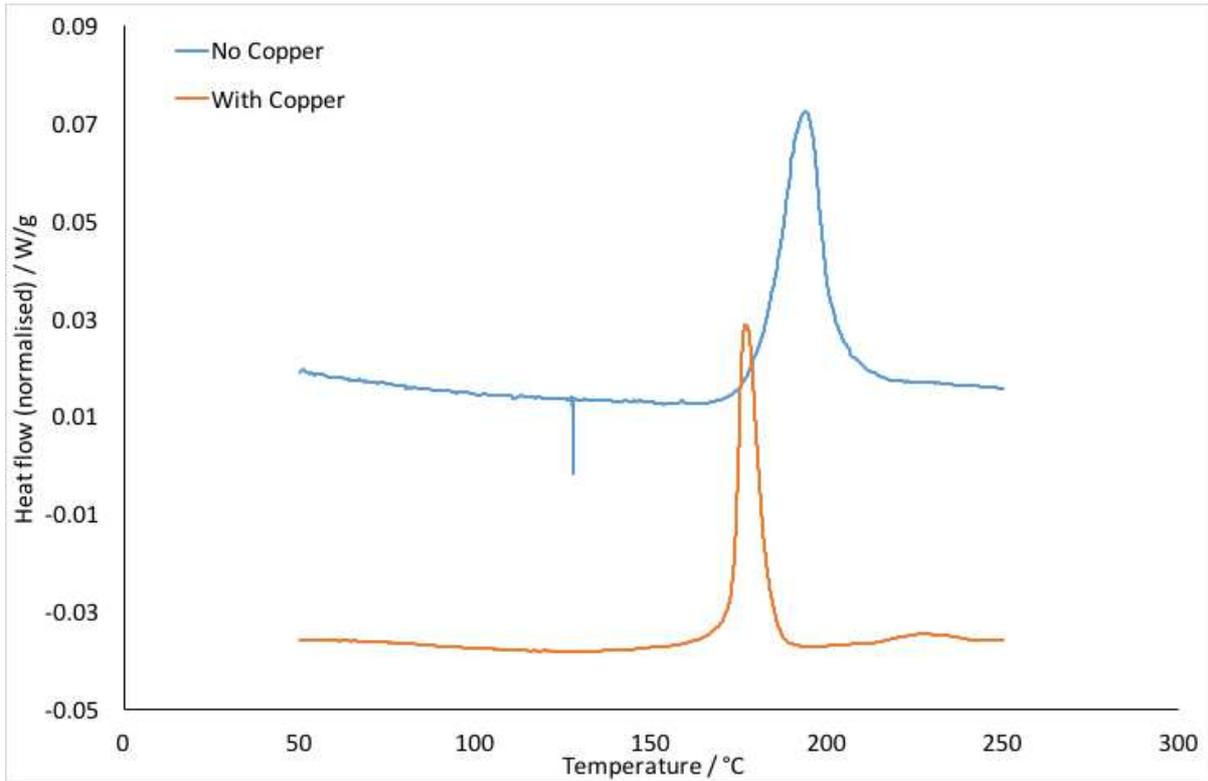
Figure 10 DSC results of DMTD with and without copper present
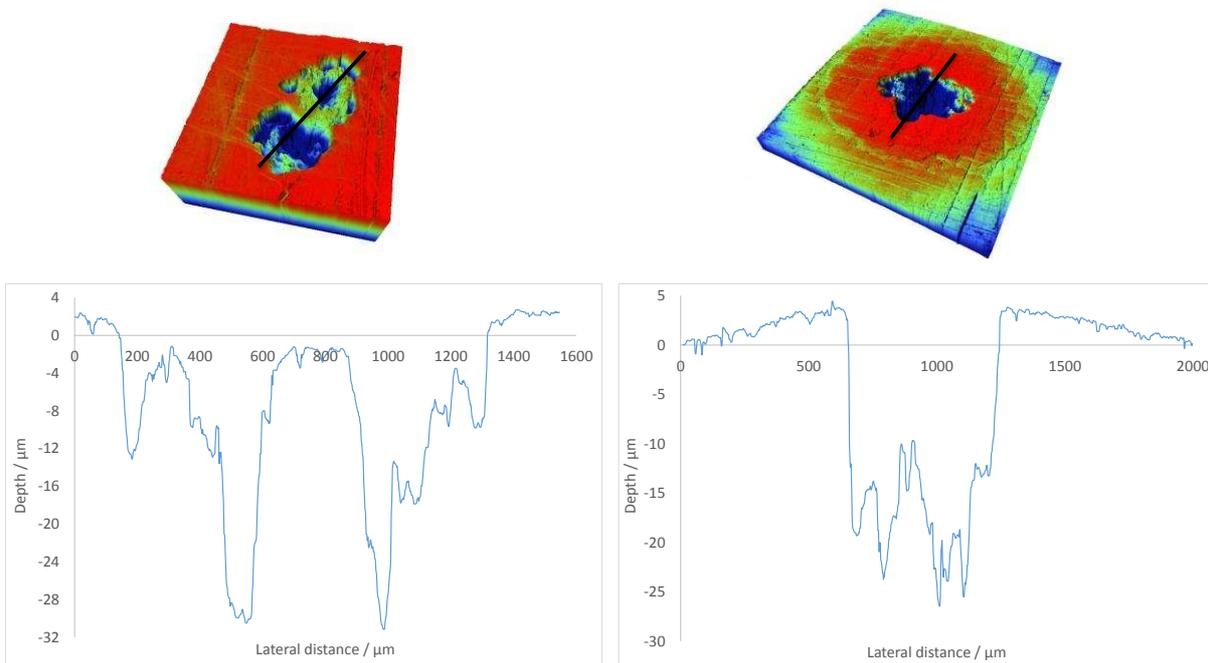
Figure 11 areas of localised pitting on the surface of the 150 ℃ sample immersed in DMTD, 3D images with position of line profiles indicated

To explore the theory that pitting was the cause of the wire breaking, White Light Interferometry was carried out on the 150 ℃ coupon, after removal of the film with acetone. The results showed the presence of two areas of severe localized pitting, as shown in Figure 11. Cross sections of the pits, also shown, show these pits were in the region of 25-30 µm deep. The presence and size of these pits suggests that the

wire breakages at this temperature could be due to pitting through the entire wire. The volume lost however is not very substantial and so explains why there was no great increase in the amount of copper measured in the end of test fluid at this temperature. Given the volume of the pits and the amount of fluid there would be an expected rise of 0.2 ppm, which would be an average of 0.1 ppm per pit. If we assume that the breakages in the wire were similar in size, then the 7 breakages would equate to around 0.7 ppm of copper. The additional copper from pitting on both the coupon surface and the wire is less than 1 ppm, explaining why no real increase in the copper level in the end of test fluid at 150 ℃ was measured. Elemental sulfur an d short chain thiols are known to be highly corrosive to copper and it is likely that the corrosion inhibitor molecule is breaking down to give such a species.

SEM images of the surfaces of coupons immersed in OBT solution are shown in Figure 12. There is little to distinguish between the surfaces at any temperature. The change in the radius of the wire tests is very small, as is the amount of copper in the end of test fluid, as shown in
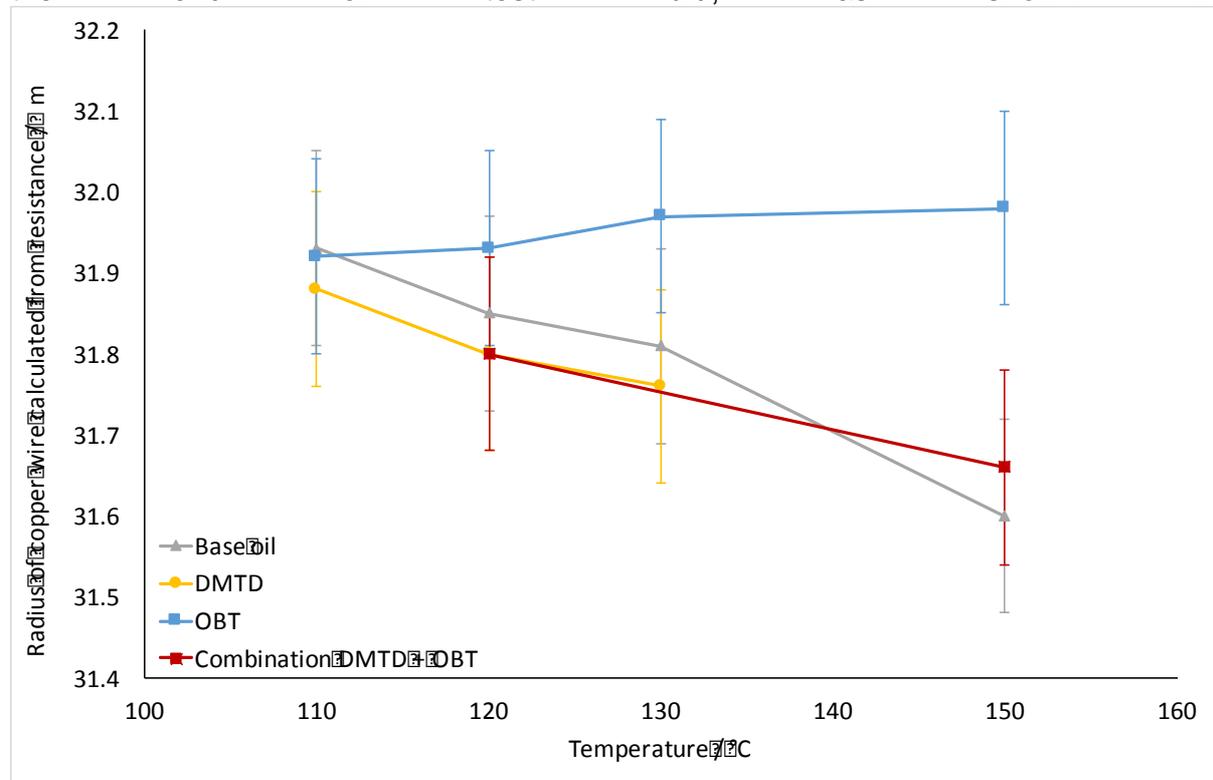

Figure **2**. This suggests that OBT is performing well. This is not surprising as OBT is a well-known copper corrosion inhibitor in aqueous systems. The tests here suggest that it also performs well in an oil-based environment.
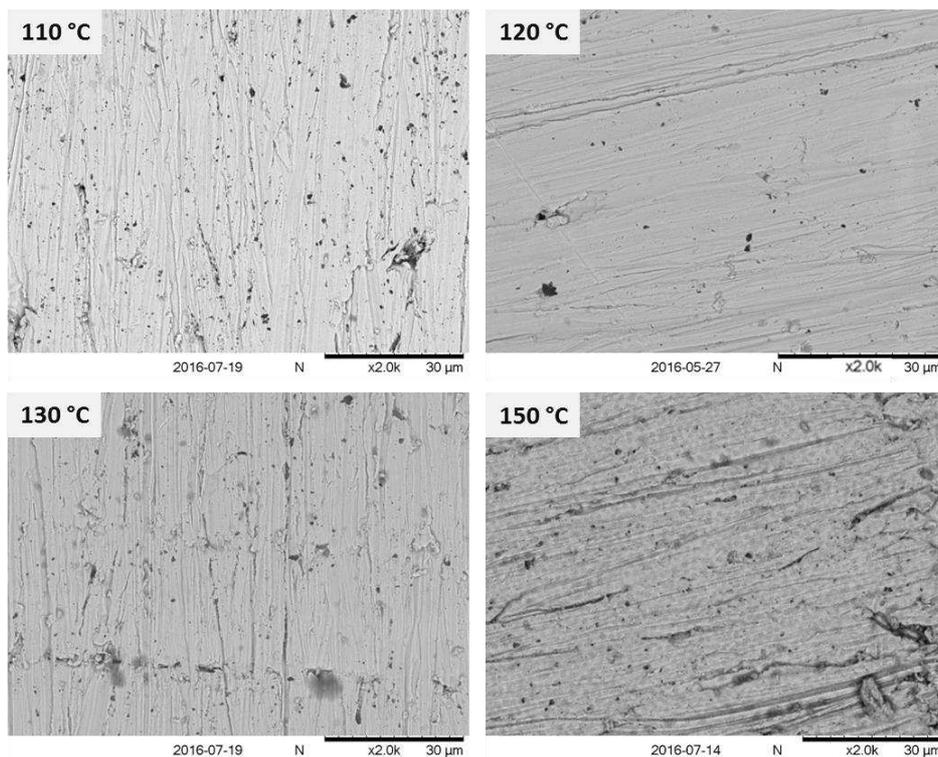
Figure 12 SEM images of the surface of copper coupons after 335 hours immersion in OBT containing test fluid at different temperatures

Figure 13 shows the XPS spectra of the surfaces at 120 ℃ and 150 ℃, with the percentage atomic concentration of the identified species shown in

Table 6.

The Cu $2s_{3/2}$ spectra tell us that the copper is in a Cu(II) oxidation state, at both temperatures, due to the satellite features present. There is a slight change in the nitrogen spectra at each temperature, but the total nitrogen percentage atomic concentration is the same. At both temperatures the presence of sulfur was detected but this is likely to be a contaminant given the levels and the lack of sulfur in the corrosion inhibitor molecule and that measured in the base oil alone. The percentage atomic concentration of sulfur was similar to that measured for coupons immersed in base oil alone.

Given the similarity in the wire results, ICP-AES results and XPS spectra, it appears that OBT interacts with the copper surface using the same mechanism at all temperatures.

The wire test method, incorporated with a copper coupon test, as described here allows the corrosion of copper to be followed in situ, without the need for supporting electrolytes, which could interfere with the interaction of the additive and the copper surface. The incorporation of the coupon allows an easier method of surface analysis.

From these results it appears that OBT may offer better protection to the copper surface than DMTD when tested alone. The interaction of these inhibitors with other additives found in ATFs is yet to be studied. Other future work may include looking at whether the addition of other additives changes the amount of corrosion measured for the copper, if the two different inhibitors interact with other additives similarly and if any synergies or antagonisms are present.
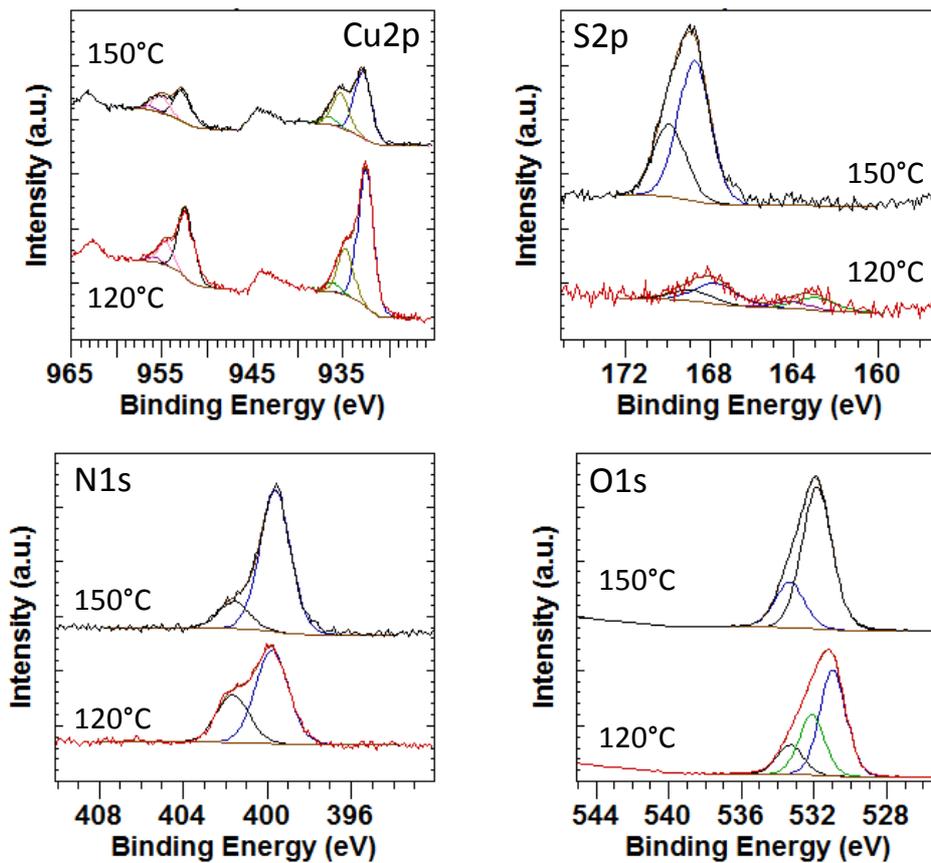
Figure 13 high resolution XPS spectra of the surface of copper coupons immersed in OBT containing test fluid at 120 ℃ and 150 ℃

Table 6 XPS analysis of coupon after immersion in OBT test solution for 335 hours

Peak	Species	120 ℃		150 ℃	
		Binding energy	% atomic concentration	Binding energy	% atomic concentration
C1s	C-C	284.78	56.44	284.82	53.05
C1s	C-O-C	286.31	9.74	286.52	12.22
C1s	O-C=O	288.46	3.80	288.68	5.78
O1s	Copper oxide/carbonate	530.96	12.64	531.77	17.31
O1s	C-O	532.12	7.99		
O1s	C=O	533.29	3.53	533.35	5.40
N1s		399.80	2.45	399.59	3.15
N1s		401.66	1.35	401.59	0.69
S2p$_{3/2}$	Cu$_2$S/Cu$_2$O	162.96	0.09		
S2p$_{3/2}$	CuSO$_4$	167.68	0.18	168.70	1.01
Cu2p$_{3/2}$	Cu$_2$O/Cu$_2$S	932.60	0.83	932.84	0.37
Cu2p$_{3/2}$	CuO	934.83	0.22	935.21	0.17
Cu2p$_{3/2}$	CuSO$_4$	936.12	0.03	936.43	0.04

4. Conclusions

From this study it is clear that the methodology provides new insights into assessing the amount of copper corrosion by lubricant additives. The change in radius of a copper wire allows the corrosion rate to be followed in situ and the nature of the change in radius data has enabled the different mechanisms of corrosion to be determined. The rapid decrease in radius of the wire in DMTD at 150℃ after 130 hours was verified as pitting on the surfaces.

The effectiveness of the protection of the corrosion inhibitors is dependent on temperature and so it cannot be assumed that an additive which shows good corrosion protection at 120 ℃ would also be protective at 150 ℃. The reverse of this is more relevant with regards the current ASTM D130 test which is currently used to assess additives. As the test is conducted at 150 ℃ an additive deemed to be poor may actually be very good at lower temperatures which are more indicative of real life working conditions.

The use of XPS has shown that the copper oxidation state for surfaces immersed in DMTD are different at 120 ℃ and 150 ℃, indicating that a differen t mechanism is occurring. This is not so for OBT as the oxidation state of the copper is the same at both 120 ℃ and 150℃.

Abbreviations

ATF	Automatic Transmission Fluid
XPS	X-ray Photoelectron Spectroscopy
FWHM	Full Width Half Maximum
SEM	Scanning Electron Microscopy
DMTD	1,3,4-thiadiazole with substituted sulfur chains
OBT	Oil soluble benzotriazole

References

[1] B. Kamchev, "Europe's Transmission of the Future," *Lubes'N'Greases Eur.* East-Africa, no. 26, 2011.

[2] ASTM D130-12, "Standard Test Method for Corrosiveness to Copper from Petroleum Products by Copper Strip Test," West Conshohocken, PA: ASTM International, 2012, DOI:10.1520/D0130-12.

[3] S. Rathgeber, R. Bauer, A. Otto, E. Peter, and J. Wilde, "Harsh environment application of electronics - Reliability of copper wiring and testability thereof," Microelectron. Reliab., vol. 52, no. 9–10, pp. 2452–2456, 2012, DOI:10.1016/j.microrel.2012.06.083.

[4] T. Ishii, N. Tsuyuno, T. Sato, and M. Masuda, "Corrosion studies of copper and aluminum interconnects exposed to automotive oils," IEEE Trans. components Packag. Technol., vol. 29, no. 1, pp. 213–221, 2006, DOI:10.1109/TCAPT.2006.870391.

[5] J. G. Cowie, "Surface Resistance Changes Due to Heat Aging of Copper and Coated Copper Alloys in Transmission and Brake Fluids," SAE Tech. Pap., no. 724, 2013, DOI:10.4271/2007-01-1384.

[6] M. P. Gahagan and G. J. Hunt, "New Insights on the Impact of Automatic Transmission Fluid (ATF) Additives on Corrosion of Copper --- The Application of a Wire Electrical Resistance Method," Int. J. Automot. Eng., vol. 7, pp. 115–120, 2016, DOI:http://doi.org/10.20485/jsaeijae.7.4_115.

[7] G. J. Hunt, M. P. Gahagan, and M. A. Peplow, "Wire resistance method for

measuring the corrosion of copper by lubricating fluids," Lubr. Sci., vol. 29, no. 4, pp. 279–290, 2017, DOI:10.1002/ls.1368.

[8] G. J. Hunt, "New perspectives on the temperature dependence of lubricant additives on copper corrosion," SAE Int. J. Fuels Lubr., vol. 10, no. 2, 2017, DOI:10.4271/2017-01-0891.

[9] P. C. Hamblin, U. Kristen, and D. Chasan, "Ashless antioxidants, copper deactivators and corrosion inhibitors: Their use in lubricating oils," Lubr. Sci., vol. 2, no. 4, pp. 287–318, Jul. 1990, DOI:10.1002/ls.3010020403.

[10] R. T. Loto, C. A. Loto, and A. P. I. Popoola, "Corrosion inhibition of thiourea and thiadiazole derivatives: A review," J. Mater. Environ. Sci., vol. 3, no. 5, pp. 885–894, 2012.

[11] A. Fateh, M. Aliofkhazraei, and A. R. Rezvanian, "Review of corrosive environments for copper and its corrosion inhibitors," Arab. J. Chem., 2017, DOI:10.1016/j.arabjc.2017.05.021.

[12] G. Hunt, "New Perspectives on lubricant additive corrosion: comparison of methods and metallurgy," SAE Int., 2018, DOI:10.4271/2018-01-0656.

[13] L. Rudnick, Lubricant Additives: Chemistry and Applications, 1st ed. New York: Marcel Dekker, 2003.

[14] D. G. Reid and G. C. Smith, "The X-ray Photoelectron Spectroscopy of Surface Films Formed During the ASTM D-130/ISO 2160 Copper Corrosion Test," Pet. Sci. Technol., vol. 32, pp. 387–394, 2014, DOI:10.1080/10916466.2011.588635.

[15] J. García-Antón, J. Monzó, J. L. Guiñón, D. Gómez, and J. Costa, "Study of corrosion on copper strips by petroleum naphtha in the ASTM D-130 test by means of electronic microscopy (SEM) and energy dispersive X-ray (EDX)," Fresenius. J. Anal. Chem., vol. 337, no. 4, pp. 382–388, 1990, DOI:10.1007/BF00322216.

[16] M. Facciotti et al., "Contact-based corrosion mechanism leading to copper sulphide deposition on insulating paper used in oil-immersed electrical power equipment," Corros. Sci., vol. 84, pp. 172–179, 2014, DOI:10.1016/j.corsci.2014.03.024.

[17] N. A. Mehanna, A. M. Y. Jaber, G. A. Oweimreen, and A. M. Abulkibash, "Assessment of Dibenzyl Disulfide and Other Oxidation Inhibitors in Transformer Mineral Oils," IEEE Trans. Dielectr. Electr. Insul., vol. 21, no. 3, pp. 1095–1099, 2014, DOI:10.1109/TDEI.2014.003909.

[18] S. Toyama, J. Tanimura, N. Yamada, E. Nagao, and T. Amimoto, "Highly Sensitive Detection Method of Dibenzyl Disulfide and the Elucidation of the Mechanism of Copper Sulfide Generation in Insulating Oil," IEEE Trans. Dielectr. Electr. Insul., vol. 16, no. 2, 2009, DOI:10.1109/TDEI.2009.4815186.